Available online at www.sciencedirect.com
ScienceDirect
Materials Chemistry and Physics 105 (2007) 20–24
MATERIALS CHEMISTRY AND PHYSICS
www.elsevier.com/locate/matchemphys

Surfactant-assisted room-temperature synthesis of CdSe nanoclusters

R. Sathyamoorthy [a,*], V. Manjuladevi [a], P. Sudhagar [a], S. Senthilarasu [a], U. Pal [b]

[a] Department of Physics, Kongunadu Arts and Science College, Coimbatore 641029, Tamilnadu, India
[b] Instituto de Física, Universidad Autónoma de Puebla, Apdo. Postal J-48, Puebla, Pue. 72570, Mexico

Received 20 July 2006; received in revised form 18 March 2007; accepted 8 April 2007

Abstract

CdSe nanoclusters of about 22 nm average size have been synthesized by a surfactant-assisted chemical method at room temperature. The as-grown nanoclusters were near stoichiometric and 70% of them were of hexagonal wurtzite crystalline phase. With undefined shapes, the crystalline nanoclusters remained arbitrarily oriented in a compact powder form. The morphology and structural behavior of the nanoclusters were studied by scanning electron microscopy and transmission electron microscopy. Thermal stability of the nanoclusters was studied by thermogravimetric analysis. Presence of very small clusters (<5 nm) in the sample revealed a blue shifted excitonic absorption peak along with the excitonic peak of bigger clusters.

Keywords: CdSe nanoclusters; Surfactant-assisted synthesis; Structure; Morphology

1. Introduction

Recently, there has been a considerable interest on the synthesis and characterization of nanocrystalline materials due to their size dependent physical and chemical properties such as work function, geometrical shape and structure, energy gap, bond length, etc. [1–5], very different from their bulk values. Nowadays nanometer size aggregates (clusters) of organic and inorganic materials are considered as promising building units for the artificial solids with the desired properties [6]. Semiconductor nanoparticles have attracted wide spread attention because of their size-dependent structural, morphological, optical and electronic properties arising from their high surface-to-volume ratio and charge-carrier confinements [7]. Synthesis of binary metal chalcogenide semiconductors of group $A^{II}B^{VI}$ in nanocrystalline form has been a rapidly growing area of research due to their important nonlinear optical properties, luminescent properties, quantum size effect and other important physical and chemical properties [8–11]. Cadmium selenide, one of the most important semiconductors in this group, finds wide range of applications like fluorescent probes [12], laser diodes [13,14], catalysis [15], solar cells [16] and biological labeling [17]. In nanocrystalline form, CdSe is of great opto-electronic interest as its band gap can be tuned across the visible spectral region by varying its particle size [18]. Different routes have been employed to synthesize cadmium selenide nanoparticles. These methods include electrochemical route [19], laser ablation [20], solid phase reaction [21] and surfactant-assisted hydrothermal method [22] among others. In this communication, we report a surfactant-assisted chemical synthesis of CdSe nanoclusters at room temperature. Nanoclusters of about 22 nm average size could be synthesized by controlling the concentration of surfactant in the reaction mixture. The nanoclusters were characterized by X-ray diffraction, thermogravimetric analysis, electron microscopy and optical absorption techniques.

2. Experimental details

2.1. Synthesis of cadmium selenide powders

All the chemicals used are of analytical grade or of highest purity available and obtained from Merck and Fluka. A suspension of cadmium oxide powder (100 mmol) was prepared in 20 ml of Triton X-100 (~24 mmol). Solution of sodium hydrogen selenide ($NaBH_4$/Se in 40 ml water) was added drop wise under constant stirring to the suspension at 40 °C (room temperature). The resulting mixture was kept under stirring for 12 h and left overnight. The product was washed repeatedly with cyclohexane and diethyl ether to remove the surfactant. The mixture was then decanted with acetone to obtain fine brown colored powder. The whole synthesis process was carried out under room temperature.

* Corresponding author. Tel.: +91 422 2642095; fax: +91 422 2644452.
E-mail addresses: rsathya59@yahoo.co.in, rsathya59@gmail.com (R. Sathyamoorthy).

0254-0584/$ – see front matter © 2007 Elsevier B.V. All rights reserved.
doi:10.1016/j.matchemphys.2007.04.008

The obtained powder was characterized by X-ray diffraction (XRD, Shimadzu XRD-6000 diffractometer), using Cu Kα radiation. The simultaneous TG and DTA thermograms were recorded using a STA 1500 version V4.30 instrument. Morphology and composition of the CdSe powder were analyzed by a scanning electron microscope (JEOL JSM-5300) attached with the EDS (Thermo Noran Super dry II) analyzer. For transmission electron microscopy (TEM), a JEOL 2010 FasTem analytical microscope equipped with Z-contrast annular detectors was used. Samples for microscopic observations were prepared by putting a drop of the powder sample dispersed in methanol and subsequent drying in vacuum. Room temperature UV–vis absorption spectra were obtained with a SHIMADZU UV-3101PC double beam spectrophotometer.

3. Results and discussion

3.1. X-ray diffraction

The XRD pattern of the prepared CdSe bulk powder is shown in Fig. 1. Most of the diffraction peaks could be indexed to pure wurtzite CdSe with lattice constants of $a = 4.30$ Å and $c = 7.09$ Å which are in good agreement with the reported bulk values (JCPDS-ICDD No. 77-2307, $a = 4.299$ Å and $c = 7.010$ Å) [22]. Along with the CdSe diffraction peaks, the traces of Se, CdO, and Cd also revealed in the XRD pattern at peak positions $2\theta = 29.59°$ and 61.6°, 32.99° and 38.48°, respectively. Presence of such undesirable peaks may be the consequences of preparative conditions. The particle size of the prepared sample was estimated using Debye–Scherer equation:

$$D = \frac{0.94\lambda}{\beta \cos\theta}$$

where D is the grain size, λ the wavelength of X-ray, β the full width at half maximum of the peak and θ is the Bragg's diffraction angle. The particle sizes estimated from different peaks are given in Table 1. EDS measurements on the prepared sample reveal the presence of Cd and Se with the atomic percentage 45.43 and 53.09, respectively, which is close to stiochiometry.

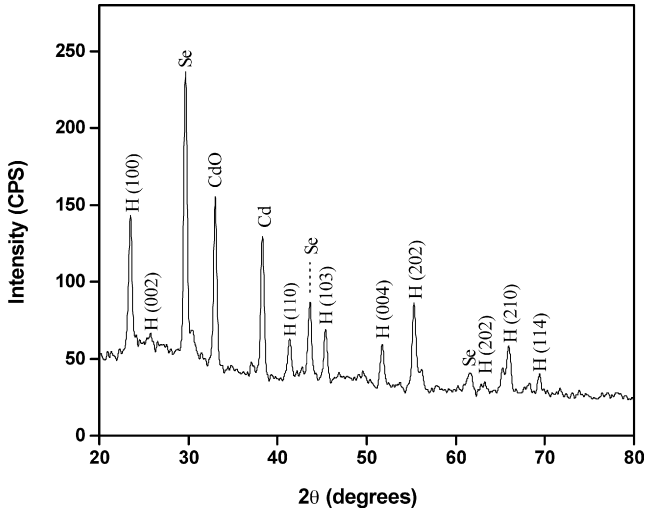

Fig. 1. XRD pattern for the bulk CdSe.

Table 1
Calculated inter-planer spacing 'd', ($h\,k\,l$) and grain size values for CdSe powder for different XRD peaks

2θ (°)	Experimental d (Å)	Standard d (Å)	$h\,k\,l$	Grain size D (nm)
23.47	3.787	3.723	1 0 0	18.96
41.32	2.183	2.149	1 1 0	23.98
51.68	1.767	1.752	0 0 4	21.45
65.90	1.416	1.407	2 1 0	21.05
69.33	1.354	1.358	1 1 4	25.88

3.2. Thermal analysis

Thermal analysis of the as-prepared bulk material was carried out in air ambient. From the thermogram presented in Fig. 2, we can observe that the sample undergoes an endothermic decomposition at about 55 °C. The weight loss at this temperature is only 0.3%, which may be due to loss of organic solvents associated with CdSe nanopowder. At 216 °C it undergoes endothermic decomposition with a mass loss equal to 3%. When the temperature is increased further, it undergoes exothermic decomposition in the range 256–487 °C, with a mass loss of about 23%. This is due to the loss of organic dispersion medium. Above 500 °C there is a gain in mass of 5%, probably due to the oxidation of cadmium selenide particles. On further heating, the oxidized product decomposes to form individual metal oxides. The weight loss of 7% above 550 °C might be due to sublimation of the oxide products at high temperature. The thermal analysis results of our CdSe powder indicate the presence of particles in the range nanometer (nm) size range. Our CdSe nanoparticles undergo decomposition below 500 °C, which is much lower than the melting (1240 °C) or decomposition (starting at 1150 °C) temperature of bulk CdSe.

3.3. Scanning electron microscopy (SEM)

Fig. 3 shows the SEM micrographs of the prepared CdSe powder for four different magnification 2000×, 6000×, 8000× and 20,000×. Formation of nanometer size clusters is clear from the micrographs. In Fig. 3A we can see the presence of scattered nan-

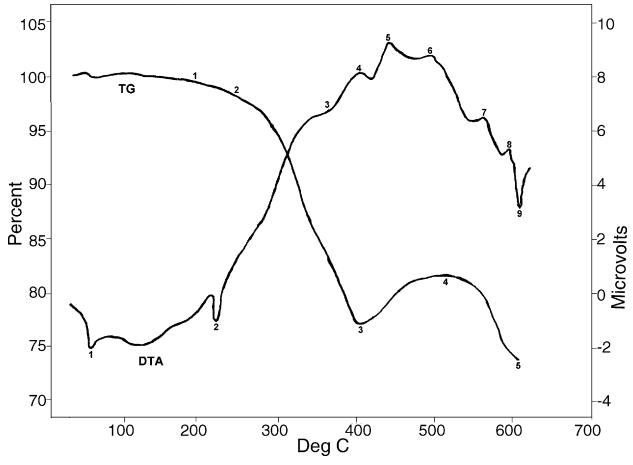

Fig. 2. TG–DTA thermogram of CdSe powder.

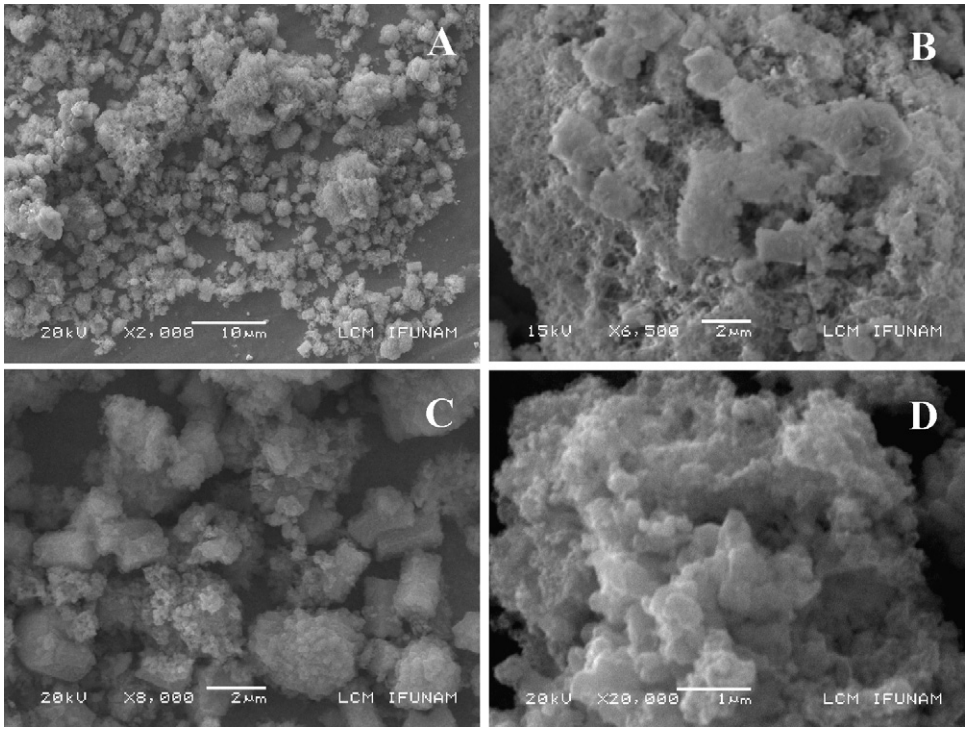

Fig. 3. (A–D) SEM micrographs of CdSe powder at different magnifications.

oclusters with a few small rod-like structures. The nanoclusters aggregate to form densely packed domains (Fig. 3B). Formation of short and wide rod-like structures can be seen easily in Fig. 3C. In its powder form, the nanoclusters remain closely packed and embedded one over other as can be seen in Fig. 3D.

3.4. Transmission electron microscopy

Typical low magnification, high angle annular dark field (HAADF) and high-resolution transmission electron microscopic (HRTEM) images of the sample are presented in Fig. 4A–C, respectively. While in Fig. 4A, formation of nanoclusters of varied size can be observed, their composition homogeneity can be observed in Fig. 4B. Formation of crystalline nanoclusters can be clearly noticed in the HRTEM image (Fig. 4C). In the figure, we can observe closely packed nanoclusters with different orientations and sizes. While most of the nanoclusters are well crystalline with hexagonal wurtzite phase, about 30% of the clusters remained amorphous. Absence or low intensity presence of the peaks like (0 0 2) and (1 0 1) in

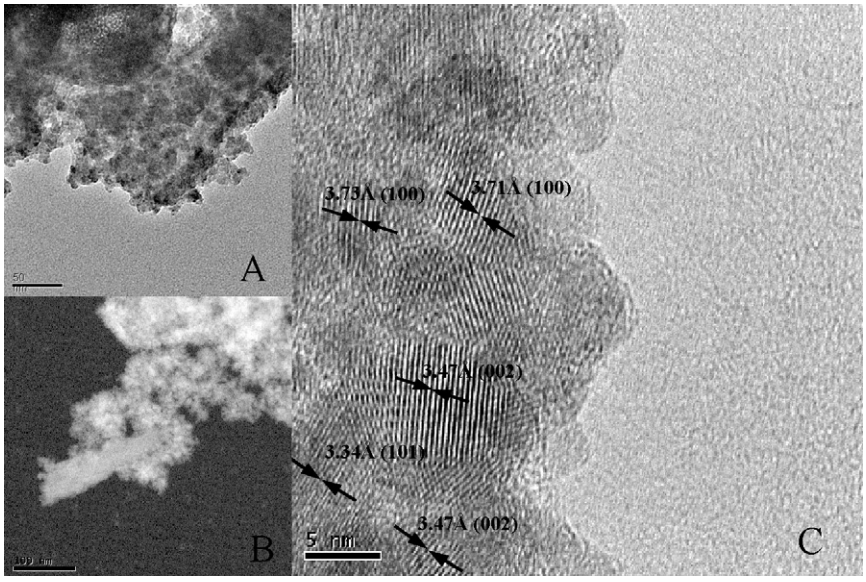

Fig. 4. Typical (A) low magnification TEM (scale bar = 50 nm), (B) HAADF (scale bar = 100 nm) and (C) HRTEM images of the powdered CdSe sample.

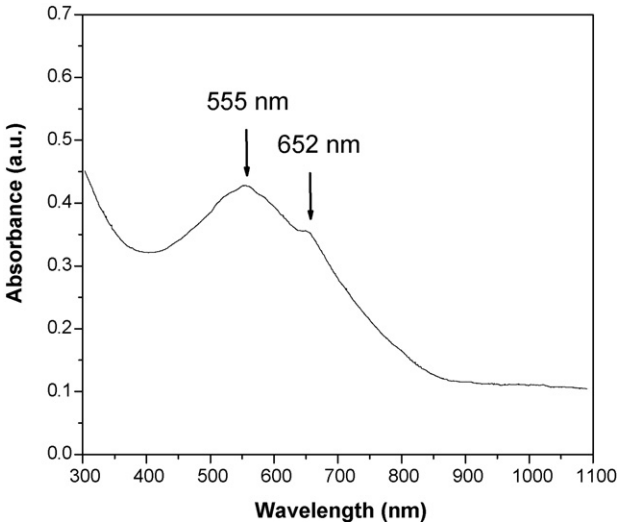

Fig. 5. UV–vis optical absorption spectrum of the CdSe powder.

the XRD spectrum (Fig. 1), which are prominent peaks in bulk CdSe, also indicates the presence of amorphous nanoclusters in the sample. Though most of the nanoclusters are of arbitrary shape, a close look on the bigger clusters can reveal that they are elongated favorably along the [0 0 2] direction. Such a directional growth of the nanoclusters and their aggregation process supports well the formation of rod-like structures seen in SEM micrographs (Fig. 3C). While the inter-planer spacing calculated from the HRTEM of individual clusters deviate significantly with their bulk values, the lattice image contrast for most of the particles with higher order lattice planes is very low. Both these effects are closely related to the presence of stacking faults in the nanoclusters [23,24].

3.5. Optical absorption in CdSe powders

Fig. 5 shows the UV–vis absorption spectrum of the obtained CdSe nanoclusters. The absorption spectrum was recorded by dispersing the powder sample in methanol through ultrasonic (3 min) treatment. The spectrum revealed two excitonic peaks at about 555 nm (2.23 eV) and 652 nm (1.90 eV), with absorption onset near 740 nm (1.676 eV). While the second excitonic peak is very close to the bulk excitonic position of CdSe, the first excitonic peak at lower wavelength indicates the presence of very small nanoclusters in the sample, where quantum size effect is prominent. Though our XRD result revealed an average particle size of about 22 nm, and SEM micrographs of about 20 nm, the high-resolution transmission electron micrographs of the sample revealed the presence of a good fraction of the clusters of even smaller sizes. We believe the appearance of lower wavelength excitonic peak in the absorption spectrum is due to the presence of smaller clusters, where a charge carrier confinement effect is in vogue. As the excitonic Bohr radius of CdSe is about 5.6 nm [25], quantum confinement effect in CdSe clusters can be observed for the clusters up to 11.2 nm size [23]. From Fig. 4C, we can observe the presence of CdSe clusters of even smaller than 5 nm in size along with the bigger ones. While the bigger clusters with bulk like optical properties revealed the second excitonic peak at about 652 nm, the smaller clusters revealed the first excitonic peak at lower wavelength. The onset of the absorption spectrum (at about 740 nm or 1.676 eV) is slightly red shifted from the bulk absorption onset (at about 712 nm, 1.74 eV). Such a red shift of the absorption onset might be due to the stoichiometric deviation of our sample. As the band gap of Se (1.5 eV) is lower than CdSe, a slight excess of Se in our sample might have caused the red shift of the band gap. It must be mentioned that the excitation on the red edge of the sample absorption reduces residual sample inhomogenities by optically selecting the largest crystallites in the distribution [25]. Therefore, the absorption onset we considered to evaluate the band edge is the band edge for the bigger clusters.

4. Conclusion

CdSe nanoclusters are synthesized through a surfactant-assisted chemical technique at room temperature. The sample contained bigger clusters of about 22 nm, and smaller clusters of less than 5 nm average sizes. While 70% of the clusters were crystalline with hexagonal wurtzite phase, the rest were amorphous. The nanoclusters preferentially grow along the (0 0 2) direction and form the basis for rod-like one dimensional nanostructure growth. Bimodal size distribution of the nanoclusters with average cluster sizes of 22 nm and less than 5 nm revealed two excitonic peaks in the optical absorption spectrum. The red shift of the absorption onset is due to the presence of Se in excess in the sample.

Acknowledgements

The authors wish to acknowledge the Secretary and the management of Kongunadu Arts and Science College for their support to carry out this work. R.S is thankful to the University grants commission, New Delhi, for awarding UGC research award. We also acknowledge the Central Microscopy Laboratory of IFUNAM, Mexico, for providing microscopy facilities used in this work.

References

[1] S.S. Kale, C.D. Lokhande, Mater. Chem. Phys. 62 (2000) 103.
[2] A. Henglein, Chem. Rev. 89 (1989) 1861.
[3] L. Brus, Appl. Phys. A 53 (1991) 465.
[4] Y. Wang, N. Herron, J. Phys. Chem. 95 (1991) 525.
[5] H. Weller, Adv. Mater. 5 (1993) 88.
[6] V.P. Biju, Y. Makita, A. Sonoda, H. Yokoyama, Y. Baba, M. Ishikawa, J. Phys. Chem. B 109 (2005) 13899.
[7] R.B. Kale, C.D. Lokhande, J. Phys. Chem. B 109 (2005) 20288.
[8] S.A. Empedocles, D.J. Norris, M.G. Bawendi, Phys. Rev. Lett. 77 (1996) 3873.
[9] M.C. Schlamp, X. Peng, A.P. Alivisatos, J. Appl. Phys. 82 (1997) 5837.
[10] M.T. Harrison, S.V. Kershaw, M.G. Burt, A.L. Rogach, A. Kornowski, A. Eychmüller, H. Weller, Pure Appl. Chem. 72 (2000) 295.
[11] H. Mattoussi, H. Leonard, R. Bashir, O. Dabbousi, E.L. Thomas, M.F. Rubner, H. Weller, J. Appl. Phys. 83 (1998) 7965.
[12] Y.-l. Yan, Y. Li, X.-F. Qian, J. Yin, Z.-K. Zhu, Mater. Sci. Eng. B 103 (2003) 202.
[13] V.L. Colvin, M.C. Schlamp, A.P. Alivisatos, Nature 370 (1994) 354.

[14] Y. Xie, Y. Qian, W. Wang, S. Zhang, Y. Zhang, Science 272 (1996) 1926.
[15] W.U. Huynh, X. Peng, A. Paul Alivisatos, Adv. Mater. 11 (1999) 923.
[16] M. Bruchez, M. Moronne, P. Gin, S. Weiss, A. Paul Alivisatos, Science 281 (1998) 2013.
[17] P.K. Khanna, R.M. Gorte, C.P. Morley, Mater. Lett. 57 (2003) 1464.
[18] R.B. Kale, S.D. Sartale, B.K. Chougule, C.D. Lokhande, Semiconductor Sci. Technol. 19 (2004) 980.
[19] D. Xu, X. Shi, G. Guo, L. Gui, Y. Tang, J. Phys. Chem. B 104 (2000) 5061.
[20] C.N.R. Rao, A. Govindaraj, F. Leonard Deepak, N.A. Gunari, M. Nath, Appl. Phys. Lett. 78 (2001) 1853.
[21] R. Coustal, J. Chim. Phys. 38 (1958) 277.
[22] M. Chen, L. Gao, J. Am. Ceram. Soc. 88 (2005) 1643.
[23] C.B. Murray, D.J. Norris, M.G. Bawendi, J. Am. Chem. Soc. 115 (1993) 8706.
[24] L.T. Chadderton, A.G. Fitzgerald, A.D. Yoffe, J. Appl. Phys. 35 (1964) 1582.
[25] M. Nirmal, D.J. Norris, M. Kuno, M.G. Bawendi, Phys. Rev. Lett. 75 (1995) 3728.